

## A Gauge-Based Analysis of Daily Precipitation over East Asia

PINGPING XIE,\* AKIYO YATAGAI,<sup>†</sup> MINGYUE CHEN,\* TADAHIRO HAYASAKA,<sup>†</sup> YOSHIHIRO FUKUSHIMA,<sup>†</sup>  
CHANGMING LIU,<sup>#</sup> AND SONG YANG\*

\*NOAA Climate Prediction Center, Camp Springs, Maryland

<sup>†</sup>Research Institute for Humanity and Nature, Kyoto, Japan

<sup>#</sup>Institute of Geographical Sciences and Natural Resources Research, Chinese Academy of Science, Beijing, China

(Manuscript received 6 April 2006, in final form 22 September 2006)

### ABSTRACT

A new gauge-based analysis of daily precipitation has been constructed on a 0.5° latitude–longitude grid over East Asia (5°–60°N, 65°–155°E) for a 26-yr period from 1978 to 2003 using gauge observations at over 2200 stations collected from several individual sources. First, analyzed fields of daily climatology are computed by interpolating station climatology defined as the summation of the first six harmonics of the 365-calendar-day time series of the mean daily values averaged over a 20-yr period from 1978 to 1997. These fields of daily climatology are then adjusted by the Parameter-Elevation Regressions on Independent Slopes Model (PRISM) monthly precipitation climatology to correct the bias caused by orographic effects. Gridded fields of the ratio of daily precipitation to the daily climatology are created by interpolating the corresponding station values using the optimal interpolation method. Analyses of total daily precipitation are finally calculated by multiplying the daily climatology by the daily ratio.

Cross-validation tests indicated that this gauge-based analysis has high quantitative quality with a negligible bias and a correlation coefficient of ~0.6 for comparisons between withdrawn station data and the analysis at a 0.05° latitude–longitude grid box. The quality of the analysis increases with the gauge network density. The mean distribution and annual cycle of this new gauge analysis present similar patterns but with more detailed structures and slightly larger magnitude compared to other published monthly gauge analyses over the region.

The East Asia gauge analysis is applied to verify the performance of five satellite-based precipitation estimates. This examination reveals the regionally and seasonally dependent performance of the satellite products with the best statistics observed for relatively wet regions. Further improvements of the daily gauge analysis are underway to increase the gauge network density and to refine the algorithm to better deal with the orographic effects especially over South and Southeast Asia.

### 1. Introduction

Substantial progress has been made in the last two decades in quantitatively documenting global precipitation. Surface gauge observations have been collected, digitalized, and quality controlled by centers in several countries (Ropelewski et al. 1985; Eischeid et al. 1991; Vose et al. 1992; Schneider 1993; Morrissey et al. 1995a). Objective techniques have been developed and applied to construct analyzed fields of precipitation over global land areas from these gauge data (Rudolf 1993, Xie et al. 1996; Dai et al. 1997; New et al. 2000;

Chen et al. 2002; Willmott and Matsuura 1995). At the same time, space-borne measurements of precipitation became available from an assortment of experimental and operational platforms. Continuous developments and refinements of retrieval algorithms have yielded operational precipitation products based on satellite observations of infrared (IR; Arkin and Meisner 1987; Susskind et al. 1997; Xie and Arkin 1998), passive microwave (MW; Wilheit et al. 1991; Spencer 1993; Ferraro 1997), and space-borne precipitation radar (PR; Kummerow et al. 2000).

Furthermore, combining information from multiple satellite sensors as well as gauge observations and numerical model outputs yielded analyses of global precipitation with stable and improved quality (Huffman et al. 1997; Xie and Arkin 1997; Hsu et al. 1997; Janowiak and Xie 1999; Huffman et al. 2001; Adler et

---

Corresponding author address: Pingping Xie, NOAA Climate Prediction Center, 5200 Auth Road, Camp Springs, MD 20746.  
E-mail: Pingping.Xie@noaa.gov

al. 2003; Xie et al. 2003; Turk et al. 2004; Huffman et al. 2004; Joyce et al. 2004). These precipitation products, often called combined or merged analyses, have been utilized in a wide range of applications, including weather/climate monitoring, climate analysis, numerical model verifications, and hydrological studies (e.g., Janowiak et al. 1998; Dai and Wigley 2000; Trenberth and Caron 2000; Lau and Wu 2001; Janowiak and Xie 2003; Roads et al. 2001; Xue et al. 2005).

One deficiency of the merged precipitation products is their quantitative uncertainty over land. Examinations of hydrological budgets over several global river basins revealed unrealistically low precipitation amounts in the merged products compared to observed runoff (Nijssen et al. 2001; Fekete et al. 2004). Over land, the magnitude of these combined products is primarily dominated by gauge observations. The underestimation of land precipitation in the gauge-based analyses, and thus the merged analyses, is attributable mostly to the combined effect of (a) sparsely distributed gauge stations located mostly over low elevation plains and (b) the lack of consideration of orographic effects that tend to produce more precipitation over locations of higher elevation (Daly et al. 1994, 2002; Adam and Lettenmaier 2003; Chen et al. 2004; Su et al. 2005; Adam et al. 2006). In addition, undercatch of precipitation, especially snowfall, by gauges due to wind effect also contributes to the negative bias of gauge observations (Sevruk 1982; Legates and Willmott 1990; Ye et al. 2004). While correction for wind effect has been performed for some gauge-based and merged analyses applying climatological adjustment factors, such as those of Legates and Willmott (1990) (e.g., Adler et al. 2003; Huffman et al. 2004), the correction procedure should be carried out for precipitation measurements of shorter accumulation periods (e.g., daily) as a function of individual synoptic events and gauge type (Ye et al. 2004).

Gauge observations play a critical role in constructing precipitation analyses over land. Among the individual inputs used to define the combined precipitation analyses, both the satellite estimates and the model predictions are indirect in nature and need to be calibrated or examined using the gauge observations in one way or another (Ebert and Manton 1998; Adler et al. 2001; McCollum et al. 2002). In addition, the extended recording period of gauge observations make them the most suitable sources from which long-term variations of precipitation may be investigated. Several precipitation climatologies have been defined over global land areas from gauge-observed monthly normals (Legates and Willmott 1990; Hulme 1991; New et al. 1999). Monthly analyses of gauge-based precipitation have

been constructed over the global land domain by several groups of scientists (Bradley et al. 1987; Willmott and Matsuura 1995; Rudolf 1993; Schneider 1993; Xie et al. 1996; Dai et al. 1997; New et al. 2000; Chen et al. 2002).

Gauge-based analyses on submonthly time scales are rarely available due to limited accessibility of corresponding station observations from many countries. Meteorological observation reports exchanged routinely through the Global Telecommunication System (GTS) include daily precipitation data from only ~6000 stations worldwide, with gaps over several regions (Ropelewski et al. 1985). The Global Daily Climatology Network (GDCN; Gleason 2002) of the National Oceanic and Atmospheric Administration (NOAA) National Climatic Data Center (NCDC) collects station observed daily precipitation from ~30 000 stations. While the GDCN gauge networks are very dense over several countries (e.g., United States), station reports are only available from 69 nations, making it impossible to generate an analysis of daily precipitation with complete spatial coverage over the entire global land areas, although gauge-based analyses of daily precipitation have been constructed on a regional basis. Up to now, such regional analyses are generated and published for North America (Higgins et al. 2000), part of South America (Shi et al. 2001), Australia (Weymouth et al. 1999), and several portions of Europe (e.g., Frei and Schär 1998; Rubel and Hantel 2001).

Accurate documentation of precipitation over East Asia is of essential importance to improved understanding of hydrometeorological processes and their long-term variations (Liu and Zheng 2004). A gauge-based precipitation dataset of high time resolution is needed to depict precipitation variations, which are dominated by the migration of monsoon systems, landfalls of tropical storms, and passage of cyclones and front systems. Such a dataset has not been available over East Asia, largely because of the limited accessibility of gauge observations of daily precipitation from various institutions of the nations over the region. As part of a joint effort among the NOAA Climate Prediction Center (CPC), the Research Institute for Humanity and Nature (RIHN) of Japan, and the Institute for Geographical Sciences and Natural Resources Research (IGSNRR) of the Chinese Academy of Science, gauge observation data of daily precipitation are being collected from several individual sources. In addition, an interpolation algorithm has been developed and the first version of the gauge-based analysis of daily precipitation has been constructed on a 0.5° latitude–longitude grid over East Asia (5°–60°N, 65°–155°E) for an extended period from January 1978 to July 2003.

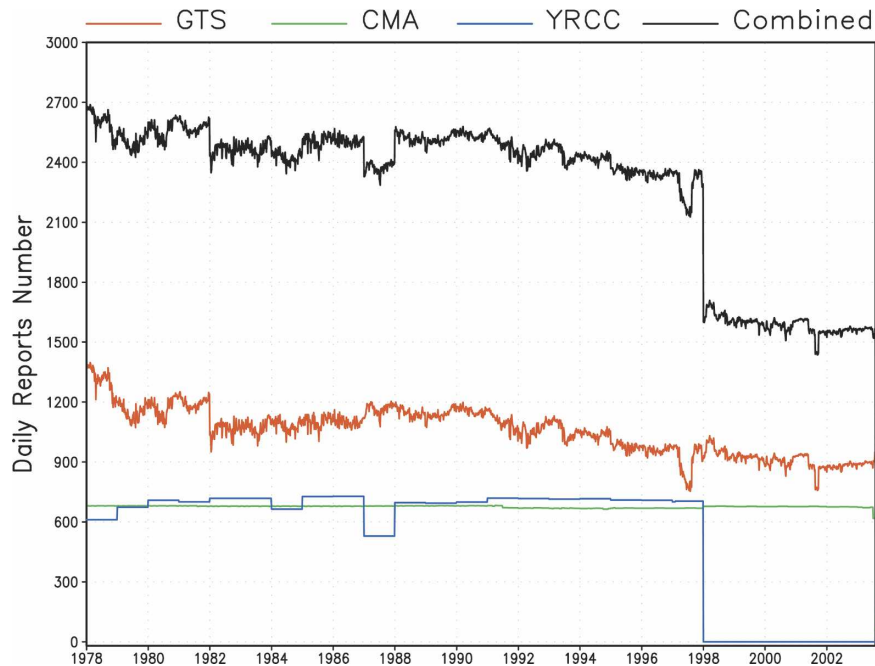


FIG. 1. Number of daily precipitation reports over the East Asia domain collected from the GTS (red), CMA archive (green), YRCC hydrological station data (blue), and their combination (black).

The objective of this paper is to describe the construction of this new gauge-based daily precipitation analysis. Section 2 describes the individual gauge datasets and the objective interpolation technique used to define the analysis, section 3 presents results of cross-validation tests and comparison with several other gauge-based analyses, section 4 illustrates applications of this new gauge dataset in verifying fine-resolution satellite precipitation estimates, and a summary is given in section 5.

## 2. Gauge data and objective analysis technique

The quality of a gauge-based precipitation analysis is a combined function of the spatial variability of the target precipitation fields, density, and configuration of the gauge network to catch the precipitation and the objective technique used to define gridded fields from the station observations (Morrissey et al. 1995b). In general, improved quantitative accuracy can be achieved through the utilization of a sophisticated interpolation algorithm and enhanced gauge observations. In constructing the gauge-based analysis of daily precipitation over East Asia, special efforts have been made to collect station observations from several individual data sources and to develop an objective analysis technique with explicit consideration to account for the orographic effects in precipitation.

### a. Input gauge data

In this study, station observations of daily precipitation from three individual datasets are used to construct the gauge-based analyses over East Asia. These are the GTS daily summary files archived by the NOAA CPC for a period from 1977 to the present; a collection of daily precipitation observations at over 700 Chinese stations archived by the China Meteorological Administration (CMA) for a period from 1951 to 2003; and the daily gauge data at over ~1000 hydrological stations from the Chinese Yellow River Conservation Commission (YRCC) for a period from the 1930s to 1997. Since most of the GTS stations are included in the CMA dataset, only daily observations from CMA and YRCC datasets are used inside China, while the GTS gauge data are used over the regions outside China.

Figure 1 presents the numbers of available daily reports from the individual data sources and their combination through the period from 1978 to 2003 for which our gauge-based analysis is constructed. Relatively stable numbers of daily precipitation reports are collected for most years during the study period. On average, observations are available at ~1000, ~700, and ~700 stations, respectively, from GTS, CMA, and YRCC. Combined, the number of daily reports reaches over 2200 for the period before 1997 when all three datasets are available and over 1500 after the YRCC

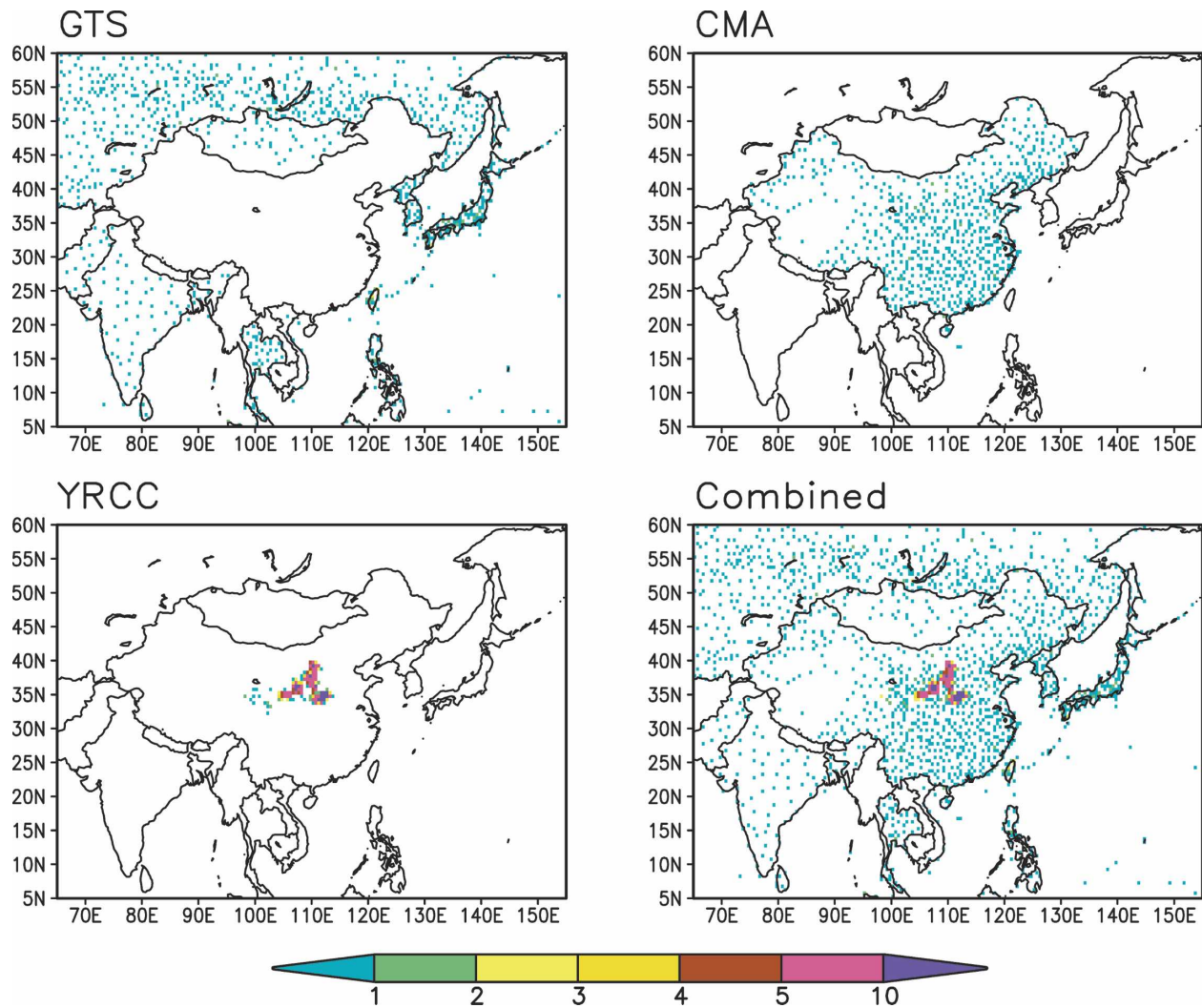


FIG. 2. Number of gauge stations in a  $0.5^\circ$  latitude–longitude grid from the three individual data sources and their combination.

dataset ends. Figure 2 shows the number of available gauges in a  $0.5^\circ$  latitude–longitude grid from the individual and the combined datasets. Reasonable gauge coverage is available over most of the land areas of the East Asia domain ( $5^\circ$ – $60^\circ$ N,  $65^\circ$ – $155^\circ$ E). The gauge network is quite dense over most of the Chinese territories while precipitation is extremely well sampled along the Yellow River with the hydrological stations. Since all of the previously published precipitation analyses over China are based on gauge observations from  $\sim 200$  GTS stations, this new gauge analysis is expected to present much improved quantitative accuracy over the region.

One major challenge in creating gauge-based daily precipitation analyses is to handle the station reports with different reporting times. The ending time for a

24-hourly precipitation accumulation differs from country to country. It is impossible to convert the original daily reports into daily values with the same reporting time everywhere without additional information of sub-daily precipitation observation, which is unavailable from most stations. Over the East Asia domain, the ending time of a day varies from 0900 UTC of the target day to 0600 UTC of the next day. While the analysis derived from these gauge reports may exhibit discontinuity across the national boundaries, it presents consistent quantitative accuracy within a country and over regions with the same daily ending time. A map is attached to the daily precipitation analysis product suite described in this paper to indicate the ending time of a daily period for the station reports used in each version of the daily precipitation analysis. Cautions are needed

in using the gauge-based analysis over the boundaries where quality of the interpolated precipitation fields is degraded.

### b. Objective technique

The selection of the objective analysis technique is a key element to improve gauge precipitation analysis accuracy. Creutin and Obled (1982) examined several well-known schemes and recommended the optimal interpolation (OI) of Gandin (1965). Bussières and Hogg (1989) compared the performance of four algorithms and concluded that the OI does the best job, while that of Shepard (1968) performs almost as well in interpolating the total amount of daily precipitation. This is confirmed by Chen et al. (2002), who repeated the intercomparison for daily, pentad, and monthly precipitation and found that the OI presents the best skill, while similar performance statistics can be achieved by other inverse-distance interpolation algorithms if the anomaly, instead of the total, is interpolated.

The overall strategy for constructing our gauge-based daily precipitation analyses is a modification of Chen et al. (2002), which is an OI-based technique originally designed for interpolation of monthly precipitation over the global land areas. While the anomalies are interpolated in Chen et al. (2002), our preliminary tests showed that interpolating the ratio between the observation and the climatology yields better results for applications to daily precipitation. This is particularly true over areas where precipitation climatology presents rapid changes in spatial distribution associated with the orographic effects (e.g., across the mountain crest of Himalaya). Magnitude of daily precipitation anomaly differs substantially at stations of wet and dry climatology, causing analysis error in interpolating the station anomaly over the region. The ratio between daily total and daily climatology, meanwhile, presents less change across the region.

The creation of the daily precipitation analysis is conducted in two steps, that is, the definition of analyzed fields of daily climatology and the construction of daily precipitation fields. Analyzed fields of daily precipitation climatology are derived from historical gauge observations of daily and monthly precipitation. First, time series of 1978–97 20-yr mean daily precipitation are calculated for the 365 calendar days for all stations with 80% or higher reporting rates. Fourier truncation is then performed for the 365-day time series of raw mean daily precipitation, and the accumulation of the first six harmonic components is defined as the daily climatology of precipitation at the stations. Fourier truncation is employed here for its ability to remove components associated with high-frequency noise. The

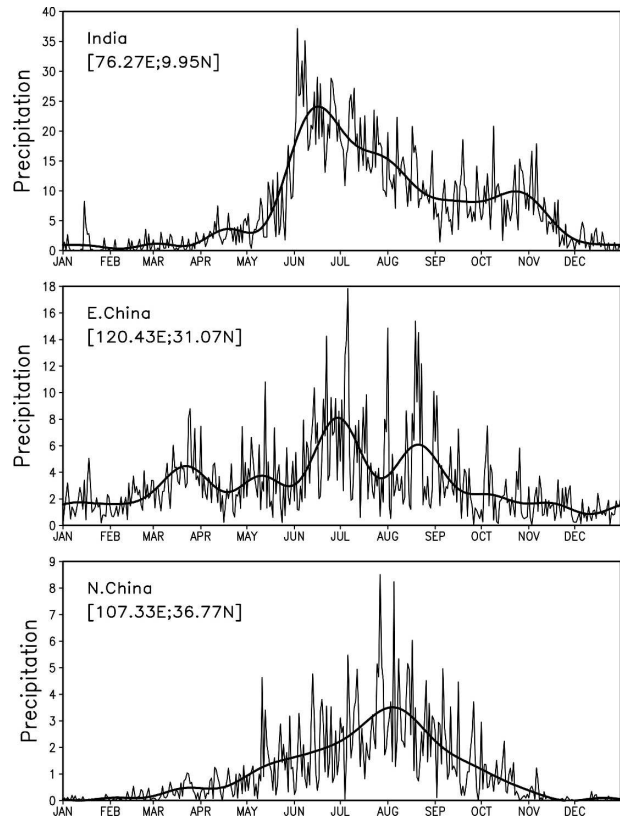


FIG. 3. Time series of 1978–97 20-yr mean daily precipitation (thin line) and accumulation of their first six harmonics (thick line) over three selected stations over (top) India (9.95°N, 76.27°E), (middle) eastern China (31.07°N, 120.43°E), and (bottom) northern China (36.77°N, 107.33°E).

number of the harmonic components included in defining the daily climatology is determined by manual examinations of the test results at  $\sim 10$  stations selected from different regions over the domain to ensure that temporal variations associated with seasonal migration, especially those of monsoons, are well reproduced. With components of 10-day or longer periods retained, the accumulation of the first six harmonics result in monthly means very close to those from the raw untruncated time series. Figure 3 presents time series of the original and truncated time series of daily precipitation climatology at three selected stations over southern India (9.95°N, 76.27°E), eastern China (31.07°N, 120.43°E), and northern China (36.77°N, 107.33°E). Seasonal variations of station precipitation associated with the monsoons, tropical storms, and frontal systems are well represented in the truncated time series while noise, caused by insufficient sampling, is removed efficiently from the original time series. Gridded fields of daily precipitation climatology are finally created by interpolating the truncated station climatology through

the algorithm of Shepard (1968), in which weighting coefficients are inversely proportional to the gauge-gridpoint distance with correction to account for the directional concentration of available gauge observations.

No orographic effects beyond those that happen to be represented in the available stations are included in defining the analyzed fields of daily precipitation climatology as described above. Gauge stations, especially those from the meteorological networks, tend to be located on plain areas with low elevation where less precipitation is observed than nearby mountainous regions (Daly et al. 1994, 2002; Chen et al. 2004). As a consequence, simple interpolation of the station observations yields an underestimation of total precipitation, especially over mountainous areas (Nijssen et al. 2001; Fekete et al. 2004). Therefore, correction for orographic effects in precipitation must be included.

While there are several approaches to correct the systematic bias (e.g., Adam and Lettenmaier 2003; Adam et al. 2006), here in this paper, a simple technique is adopted to adjust the analyzed fields of daily climatology by published monthly precipitation climatology with orographic consideration. Analyzed values of daily climatology are scaled by the monthly climatology so that the accumulation of the daily climatology is in close agreement with the monthly climatology, while the temporal variations in the original daily climatology time series are retained. To this end, monthly averages of the daily climatology are calculated for the 12 calendar months. The scaling factor for a calendar day is then computed as the ratio between the weighted mean of the monthly climatology with orographic consideration and that of the monthly averages from the unadjusted daily climatology for a 3-month period centered at the month of the target day. The weight for each of the 3 months is inversely proportional to the interval between the target calendar day and the center of the month. Similar methods are applied by several groups to correct orographic effects in daily precipitation over the United States (Schaake et al. 2004).

Over China and Mongolia, the Parameter-Elevation Regressions on Independent Slopes Model (PRISM) monthly precipitation climatology created by Daly et al. (1994, 2002) is employed to correct the orographic effects. Widely used in hydrological and meteorological studies as a standard of regional precipitation climatology, the PRISM defines monthly precipitation climatology through locally established empirical relationships between rainfall and elevation. Station climatologies (1961–90 normals) at over 2600 stations are used in defining PRISM over China, more than 10 times those used in other published climatologies.

The monthly climatology of Chen et al. (2002) is used outside China and Mongolia where the PRISM is not available. Although orographic effects are not explicitly incorporated in Chen et al. (2002), analyzed fields of monthly precipitation climatology over the region are defined by interpolating station long-term means observed by a very dense gauge network. For example, observations at over 3000 stations are included to define the monthly precipitation climatology over India, while daily reports are available from only ~200 stations. Interpolation of observations from a dense network yields spatial distributions that better represent orographic effects. The station long-term means used in Chen et al. (2002) to compute the analyzed fields of monthly climatology are defined for gauges with 10-yr or longer records during a 40-yr period from 1951 to 1990. Although raising the minimum years of observations required in calculating the long-term mean improves the quantitative accuracy and stability at the station locations, it also reduces the number of qualified stations and thereby degrades the spatial representativeness of the resulting analyzed fields of monthly climatology. Willmott et al. (1996) and Hulme and New (1997) both concluded that including additional stations yields more improvements than the degradation caused by reducing the number of years for defining the climatology.

Shown in Fig. 4 are adjusted precipitation climatology for July (top) and the topography over the East Asia domain (bottom). In addition to bands of heavy rainfall along the major mountain ranges over South and southeastern Asia, enhanced precipitation is also observed over mountainous areas over China. A line of precipitation with medium intensity is depicted along the northern slope of the Tian Shan mountain range over northwest China, while only a trace amount of precipitation is assigned over the desert areas nearby.

The second step of our interpolation algorithm involves the construction of the daily precipitation analyses. To this end, analyzed fields of the ratio of daily precipitation total to the daily climatology are created by interpolating the corresponding station values, defined as the ratio of daily observation at a station to the daily climatology at the grid box at the gauge location. The OI algorithm of Gandin (1965) is applied, following Chen et al. (2002). Analyses of total daily precipitation are finally calculated by multiplying the analyzed daily climatology with the daily ratio. In creating the products, the analysis is first produced on a  $0.05^\circ$  latitude–longitude grid over the entire East Asia domain. Computing analyzed values at a fine resolution enables improved correction of the orographic effects, which exhibit rapid changes with elevation (Daly et al. 1994).

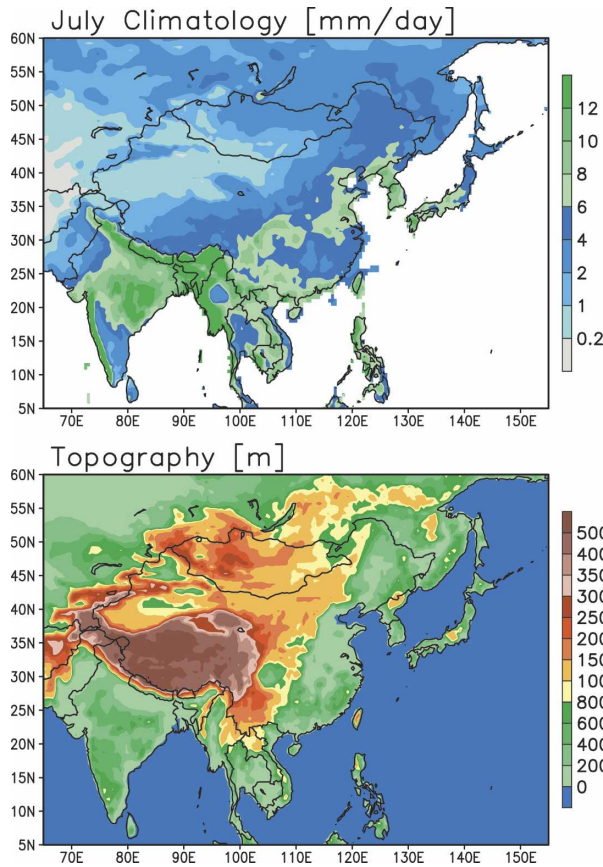


FIG. 4. (bottom) Topography (m) and (top) July precipitation climatology ( $\text{mm day}^{-1}$ ) over the East Asia defined in this study by adjusting the truncated daily precipitation climatology against the PRISM monthly climatology of Daly et al. (1994, 2002) and the monthly climatology of Chen et al. (2002).

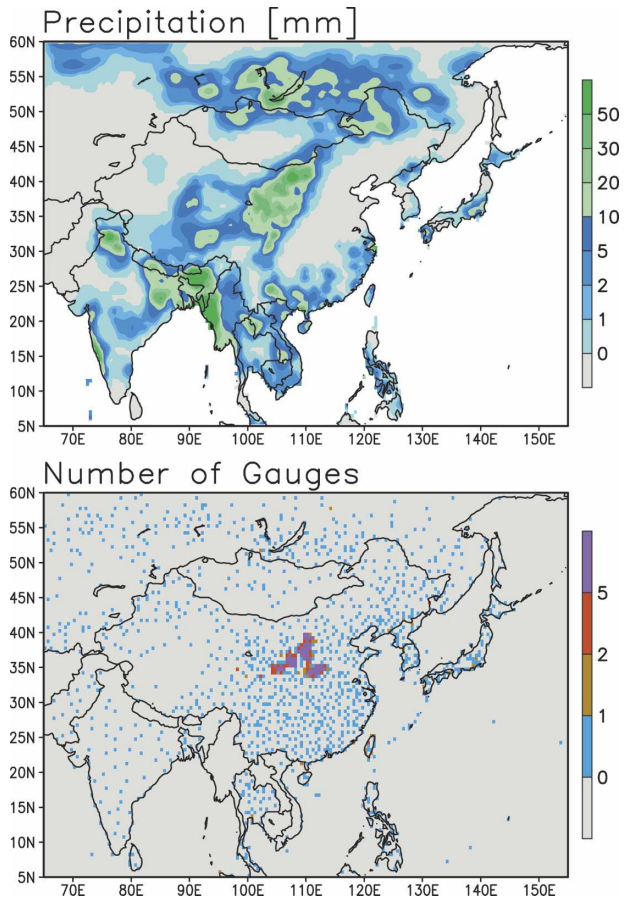


FIG. 5. (top) Analyzed field of daily precipitation and (bottom) number of station reports available in a  $0.5^\circ$  latitude–longitude grid for 14 Aug 1997.

In addition, this practice makes it easy to generate analyses at various grid resolutions for different applications. In this work, gauge-based analyses at a  $0.5^\circ$  latitude–longitude resolution are constructed by integrating the values at a  $0.05^\circ$  latitude–longitude grid and using them as final output to our users.

Here in our approach, the ratio between the station daily observation and the daily climatology at the grid box at the gauge location, instead of the daily climatology of the station itself, is interpolated and utilized to calculate the analyzed fields of daily precipitation. This practice allows us to include station observations from many more stations for which data records are not sufficient to permit the definition of a daily climatology, improving the spatial representativeness of the resulting analyses. At locations where gauge data are available, the long-term mean of the daily analyses defined this way will converge at the station’s climatological values, which are very close to those of the PRISM climatology (Daly et al. 2002). At grid boxes with no

gauge observations, the analyzed values of daily precipitation are interpolated from nearby station observations with orographic adjustments through the employment of daily climatology.

### 3. The 26-yr gauge analyses

#### a. Construction of the daily analyses

The algorithm described in the previous section is applied to construct the gauge-based analysis of daily precipitation on a  $0.5^\circ$  latitude–longitude grid over East Asia ( $5^\circ$ – $60^\circ$ N,  $65^\circ$ – $155^\circ$ E) for a 26-yr period from January 1978 to July 2003. In addition to the analyzed fields of daily precipitation, the number of gauge reports available at each  $0.5^\circ$  latitude–longitude grid box is also included as a proxy index for the analysis quality. For convenience, we refer to this new product as the EA gauge analysis in the following discussions.

Figure 5 illustrates an example of the EA gauge analysis for 14 August 1997. Zones of heavy rainfall are

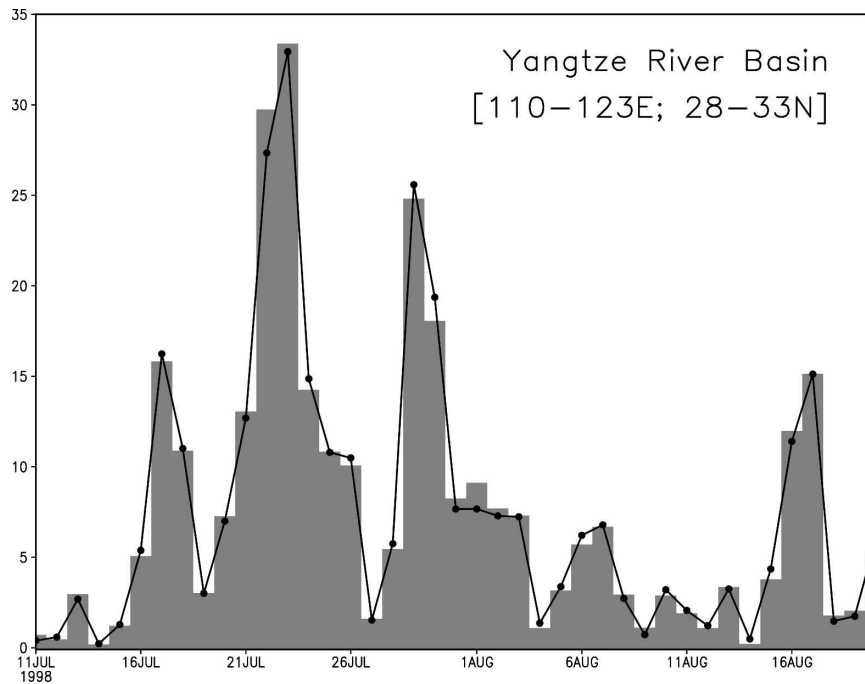


FIG. 6. Time series of mean daily precipitation observed by  $\sim 75$  gauges (bar) over the Yangtze River basin ( $28^{\circ}$ – $33^{\circ}$ N,  $110^{\circ}$ – $123^{\circ}$ E) and that from our daily analysis at the gauge locations (line) from 11 Jul to 20 Aug 1998.

observed over the Western Ghats, southern slope of the Himalayas, Bangladesh, and the coastal region of Burma. Bands of precipitation associated with the passage of frontal and cyclone systems appear over central China and southeastern Russia. Also visible is rainfall of medium intensity over southeastern China caused by scattered convection, which is typical over the region during August. Figure 6 presents the time series of mean daily precipitation observed by  $\sim 75$  gauges (bar) over the Yangtze River basin ( $28^{\circ}$ – $33^{\circ}$ N,  $110^{\circ}$ – $123^{\circ}$ E) and that from our daily analysis at the gauge locations (line) during the 1998 summer season. Day-to-day variations of precipitation as shown in the time series of the gauge observations are well captured in the gauge-based analysis. Episodes of heavy rainfall pass through the river basin in intervals of  $\sim 7$  days, contributing to one of the greatest flooding events in decades over the region. Differences between the mean daily precipitation from the station observations and that from the analyses are usually less than  $1 \text{ mm day}^{-1}$ .

#### b. Cross-validation tests

To examine the quantitative accuracy of the gauge-based analysis, cross-validation tests were conducted for the interpolation algorithm developed in this study. Daily precipitation reports for the 10% randomly se-

lected stations are withdrawn and reports for the remaining 90% of the stations are used to create the gauge-based analyses as described in section 2b. This process is repeated 10 times so that each station is withdrawn once. The withdrawn gauge observations are then compared with analyzed daily precipitation at the  $0.05^{\circ}$  latitude–longitude grid box, where the gauge is located to assess to what extent the analyzed values may represent the mean magnitude and temporal variations of station daily precipitation. Comparisons are conducted separately for the three groups of gauges, the GTS, CMA, and YRCC, to get insight into how the EA gauge analyses perform over different portions of the target domain.

Table 1 presents the comparison results for a 365-day period of 1997. The biases are very small for all station groups, indicating that the daily analysis has very good overall magnitude agreements with the observations.

TABLE 1. Cross-validation results for 1997.

Stations	Mean (mm)	Bias (mm)	Correlation
ALL	1.972	0.036	0.594
GTS	2.590	0.086	0.504
CMA	2.211	−0.009	0.716
YRCC	0.913	0.005	0.860

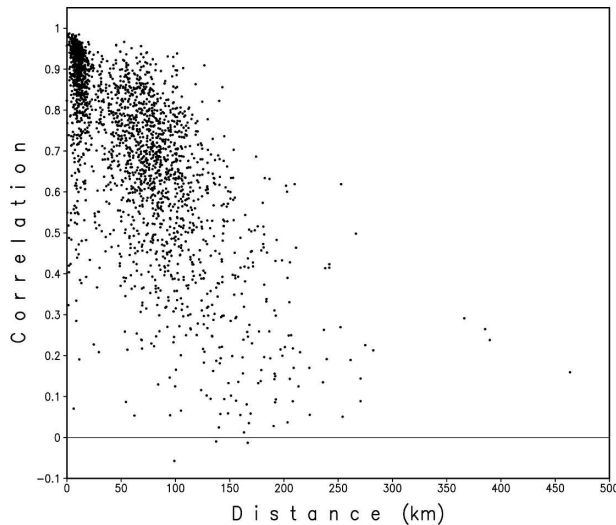


FIG. 7. Scatterplots between the station daily precipitation–analysis correlation at a withdrawn station and the distance from that station to the closest gauge with daily reports. Correlation is calculated for 365 days of 1997.

The correlation between the analyzed daily precipitation and the withdrawn (independent) gauge observations is 0.504 for the GTS stations, which are sparsely scattered outside China, while it reaches 0.860 for the YRCC stations that are very densely distributed along the Yellow River. Overall, the correlation for all stations combined is 0.594, suggesting good performance of the analyses in representing variations of daily precipitation on a spatial scale of  $0.05^\circ$  latitude–longitude.

Dependence of the performance of the gauge-based analyses on gauge network density is further explored by comparing the statistics for grid boxes with various network densities. For this purpose, serial correlation between the daily analyses and corresponding gauge observations at each withdrawn station is calculated for the 365-day period of 1997 for each of the withdrawn stations. Figure 7 presents the scatterplot between the analysis–gauge observation correlation and the distance from the  $0.05^\circ$  latitude–longitude grid box to the closest gauge from which observations are available. It is very clear that quality of the analysis improves as the gauge network becomes denser. The correlation at a grid box is smaller than 0.6 when the closest gauge station is more than 150 km away, while it may reach 0.9 or higher if precipitation reports are available for interpolation from within 50 km. The performance of the analysis is influenced by other factors (e.g., spatial scale of the precipitation system) as well, and the correlation calculated in the cross-validation presents considerable variations for locations with similar gauge network density. Most of the dots in Fig. 7 with distance shorter than

30 km represent results for stations over the Yellow River basin where gauges are very densely distributed. In consideration of the gauge location map shown in Fig. 2, it is clear that the current version of our East Asia gauge analysis should exhibit quite good performance over eastern China, Korea, Japan, and southern Russia, while quantitative reliability will be less desirable over the Tibet Plateau, Burma, and Afghanistan where gauge networks are very sparse.

One important statistic of precipitation fields is the probability density function (PDF) of precipitation intensity. In general, interpolating point observations yield analyzed fields with reduced PDF for both high and low (no rain) precipitation amounts compared to that of the original station observations, especially for regions of sparse gauge networks. Examining the fidelity of the PDF for analyzed precipitation fields, however, is not an easy task. The PDF for gauge observations, which measure precipitation at a point, is supposed to be different from that for the analyzed values, which represent precipitation averaged over a grid box. Without additional information (e.g., observations from a very dense gauge network, estimates from reliable remote sensing tools) it is very difficult to define the ground truth for the PDF for mean precipitation over the target grid boxes to which the analyzed analyses may be compared. In this study, no examination has been performed for the PDF of our gauge-based daily precipitation analysis. Cautions are needed in utilizing our dataset for applications, such as verifying the PDFs of model-generated or satellite-derived precipitation fields.

### c. Comparison with other gauge-based datasets

The spatial distribution and temporal variability of precipitation observed in our gauge-based East Asia daily analysis are investigated and compared to three sets of widely used gauge-based monthly precipitation datasets, including the analyses of the Global Precipitation Climatology Centre (GPCC; Rudolf 1993; Schneider 1993), the University of East Anglia Climate Research Unit (CRU; New et al. 1999), and the University of Delaware (UDE; Willmott and Matsuura 1995). Since no published products of gauge-based analyses of daily precipitation over the East Asia domain are available, our comparison with monthly analyses here will focus on the annual mean and mean annual cycle of precipitation to provide potential users with information on the quantitative differences between our daily products and the selected monthly datasets. Comparisons are conducted on the East Asia domain for a 12-yr period from 1986 to 1997 for which all of the datasets involved are available. All analyses

have been integrated to a grid of  $1.0^\circ$  latitude–longitude, the lowest spatial resolution available from the data sources.

While large-scale distribution patterns of the 12-yr annual mean precipitation are very similar in all of the four gauge-based datasets, our EA gauge analysis presents more details in smaller-scale features thanks to a denser gauge network used in this study (Fig. 8). Gauge observations from over 1400 Chinese stations are utilized in constructing our EA gauge analysis, compared to less than 200 stations in the three monthly gauge datasets. Overall, our EA gauge analysis exhibits a slightly larger amount of precipitation over the mountainous areas of southeastern China and along the northern slope of the Tian Shan mountain range over northwest China (right panels in Fig. 8), a reflection of the bias correction for the orographic effects in our analysis. The rainband along the west slope of the Western Ghats over India is narrower in our analysis due to a denser gauge network and an improved algorithm, which interpolates the ratio of the daily observation to the climatology instead of the total observations. In the CRU and UDE datasets, heavy rainfall spreads across the Himalayas into the southern part of the Tibet Plateau, an artifact not supported by station data over the region (not shown).

One of the potential applications of fine-resolution gauge precipitation datasets is to force hydrological models (e.g., Ma and Fukushima 2002). For this purpose, the 1986–97 12-yr mean annual cycle of monthly precipitation over two major Chinese river basins, the Yellow River ( $32^\circ$ – $43^\circ$ N,  $95^\circ$ – $123^\circ$ E) and the Yangtze River ( $28^\circ$ – $33^\circ$ N,  $110^\circ$ – $123^\circ$ E) basins, are defined for the EA analysis and the three monthly gauge datasets. Over the Yellow River basin (Fig. 9, upper panel), all of the four gauge-based datasets show a single peak annual cycle with the maximum of  $\sim 3.2$  mm day $^{-1}$  observed at July. Small differences of  $\sim 5\%$ – $10\%$  are observed in the magnitude of precipitation among the datasets examined here especially during warm seasons, with our EA analysis presenting the largest values throughout the year. Over the Yangtze River basin in southern China (Fig. 9, bottom panel), annual cycle of basinwide mean precipitation reaches its maximum ( $\sim 7.0$  mm day $^{-1}$ ) in June during the active phase of the Meiyu (Baiu) monsoon season. Similar to that over the Yellow River basin, the EA gauge analysis exhibits a slightly larger amount of precipitation for most months of the year especially during the monsoon period (June and July). For both the Yellow River and the Yangtze River basins, differences among the precipitation datasets are smaller during cold seasons (September–March). The relatively heavier rainfall in the EA gauge

analysis over the two river basins is a combined effect of the utilization of station reports from a denser gauge network and an improved algorithm with consideration of orographic effects. In particular, over the Yellow River basin, in addition to the gauge stations included in the Chinese meteorological observation network, daily precipitation reports from  $\sim 700$  hydrological stations along the river are used in the interpolation. Many of these hydrological stations are located over mountainous regions with heavier rainfall than nearby plain regions where gauges of meteorological network are usually placed, contributing to the larger amount of precipitation in our analysis. While it is important to quantify the contributions of the different input gauge reports and interpolation algorithms to the differing analyzed fields of precipitation, we are unable to carry out the examination in this work due to the unavailability of the input data and objective algorithms for the three other precipitation products.

#### 4. Applications

Construction of the high-resolution EA daily gauge analysis has made it possible to conduct quantitative examinations of precipitation over the region in a variety of applications. Recently, Yatagai et al. (2005) applied this new gauge analysis to examine the precipitation fields generated by the high-resolution global model of the Japanese Meteorological Agency (JMA). Here as an example, we verify the performance of five satellite-based products of high-resolution precipitation estimates by comparison against our new gauge analysis. The satellite products to be examined here include the NOAA CPC morphing technique (CMORPH; Joyce et al. 2004), the Tropical Rainfall Measuring Mission (TRMM) precipitation product 3B42, version 6 and its real-time version 3B42RT, version 2003 (hereafter, 3B42 will refer to version 6 and 3B42RT will refer to version 2003) (Huffman et al. 2004, 2007) of the National Aeronautics and Space Administration (NASA) Goddard Space Flight Center (GSFC), the Naval Research Laboratory (NRL) satellite precipitation estimates (Turk et al. 2004), and the Precipitation Estimation from Remotely Sensed Information using Artificial Neural Networks (PERSIANN) developed by Hsu et al. (1997) and Sorooshian et al. 2000 of the University of California at Irving. Satellite-based precipitation estimates depict the distribution and evolution of atmospheric systems with fine time/space resolution and seamless coverage over most of the globe. Examinations of these satellite products provide critical information on their performance upon which further improvements may be made and strategy to combine

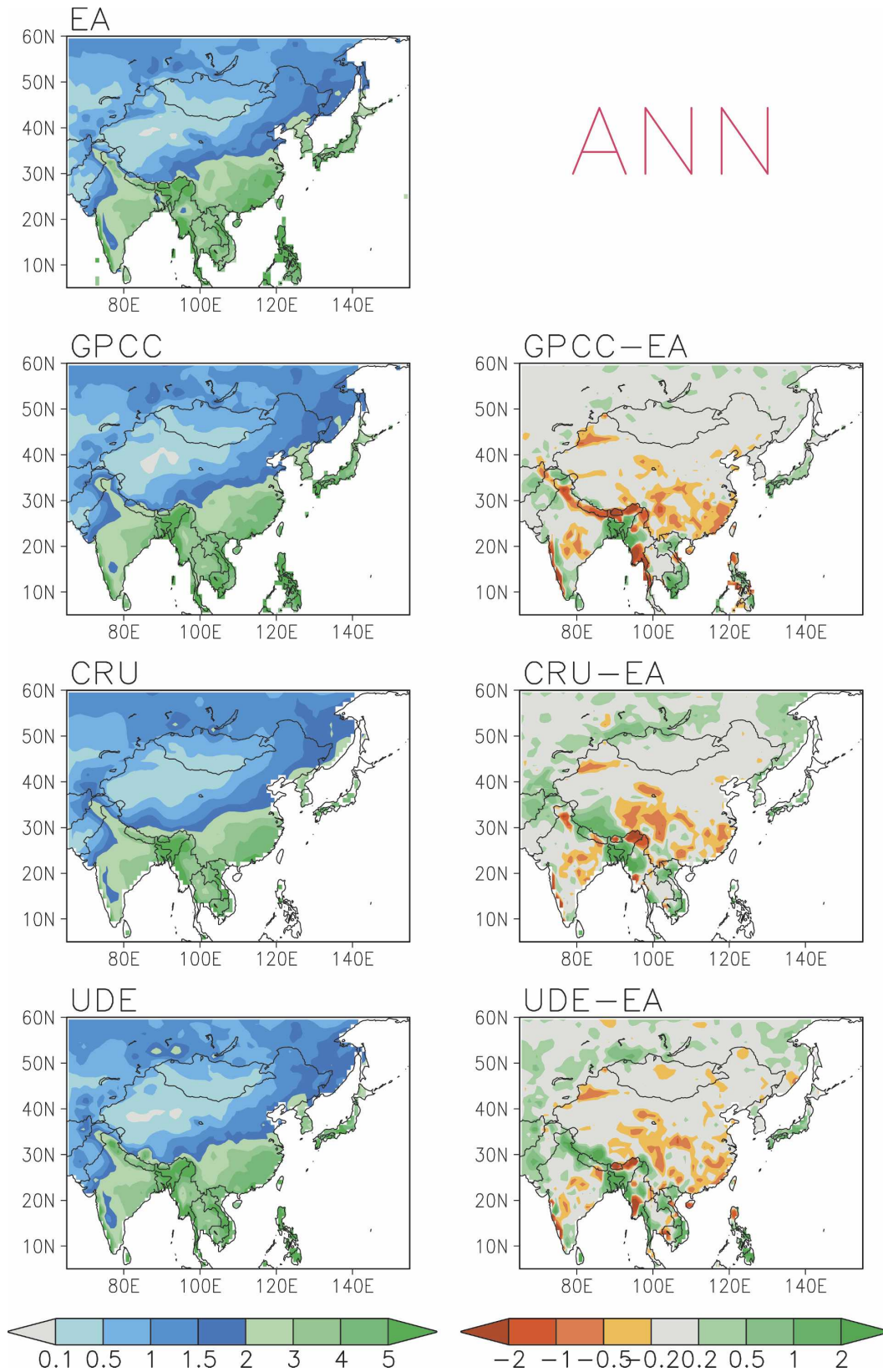


FIG. 8. Mean annual precipitation ( $\text{mm day}^{-1}$ ) for an 11-yr period from 1986 to 1997 as defined by gauge-based precipitation analyses of (top left) (i) our product described in this paper (EA), (left second from the top) (ii) GPCC, (left third from top) (iii) CRU, and (left bottom) (iv) UDE. (right) Differences between the GPCC, CRU, and UDE with our EA analysis.

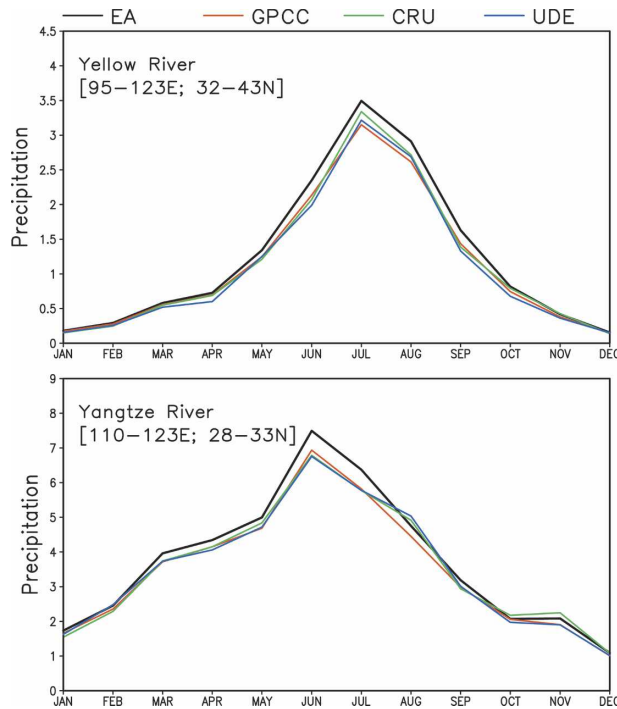


FIG. 9. Annual cycle of 1986–97 mean monthly precipitation over the (top) Yellow River (32°–43°N, 95°–123°E) and (bottom) Yangtze River (28°–33°N, 110°–123°E) basins as calculated from gauge-based analyses of EA (black), GPCC (red), CRU (green), and UDE (blue).

them with other observations (such as gauge-based analyses) may be designed (Sorooshian et al. 2000; McCollum et al. 2002; Ebert et al. 2007).

Creation of precipitation estimates on high time/space resolution over the globe requires combined use of less physically based but frequently available infrared observations from geostationary satellites and the physically based but infrequently sampled MW measurements aboard low-orbit platforms. In the NRL, PERSIANN, and TRMM 3B42RT, a regionally dependent and temporally changing relationship between precipitation amount and IR brightness temperature is established using collocated MW and IR observations, assuming that the MW-based estimates are accurate in representing surface precipitation. In the NRL and the TRMM 3B42RT algorithms, this relationship is defined by matching the PDFs of the IR and MW observations, while in the PERSIANN, it is carried out through an adoptive neural network system (Turk et al. 2004; Hsu et al. 1997; Huffman et al. 2004). Furthermore, in the TRMM 3B42RT, the IR-based precipitation estimates are combined with the MW measurements to achieve better quantitative accuracy especially over extratropical regions (Huffman et al. 2004).

A different approach is adopted in the CMORPH to

generate fine-resolution precipitation estimates from satellite observations. Consecutive geostationary IR observations are utilized to compute advection vectors of cloud and precipitation systems over the globe. These advection vectors are then used to interpolate the infrequent MW measurements aboard polar-orbiting satellites by “moving” the precipitation systems observed by the MW measurements along the advection vectors in the combined time–space domain. Fields of instantaneous precipitation rate can be created in 30-min intervals on a spatial resolution of 8 km × 8 km over the globe from 60°S to 60°N (Joyce et al. 2004).

All of the four products (CMORPH, TRMM 3B42RT, NRL, and PERSIANN) described above are based *solely* on satellite observations. The TRMM 3B42 goes one step further by taking into account the information from gauge observations. Generated on a postprocessing mode, the TRMM 3B42 is defined by adjusting an all-satellite 3-hourly precipitation product that is similar to the real-time dataset of 3B42RT through the GPCC gauge-based monthly precipitation analysis to reduce the bias inherent in the satellite-based estimates (Huffman et al. 2007). A better performance of 3B42 is expected due to the combined effect of the bias correction procedure and the fact that more MW-based estimates are used in the all-satellite product than those in its real-time counterpart of 3B42RT.

The input satellite data used to generate the fine-resolution precipitation differ for the five techniques. For the time period for which our comparison is performed (January–July 2003), MW-based precipitation estimates from TRMM Microwave Imager (TMI) and Special Sensor Microwave Imager (SSM/I) aboard three Defense Meteorological Satellite Program (DMSP) satellites are used in the production of TRMM 3B42RT, NRL, and PERSIANN, while those from the Advanced Microwave Sounding Unit (AMSU) are included in addition in defining the TRMM 3B42, NRL, and the CMORPH. The AMSU estimates used in creating the NRL product are *not* calibrated against the TRMM TMI estimates as in CMORPH and TRMM 3B42RT and do not include those over 10 pixels on either side of the scan swath. In general, incorporating additional input data with intercalibration yields stable and improved performance of the precipitation products.

Quality control of the input data is critical in ensuring reliable performance of the final products of fine-resolution precipitation. Particularly important is the screening of the MW observation pixels contaminated with surface snow/ice that produce strong scattering signals mistaken as those from precipitating clouds if the pixels are not identified and removed. In the

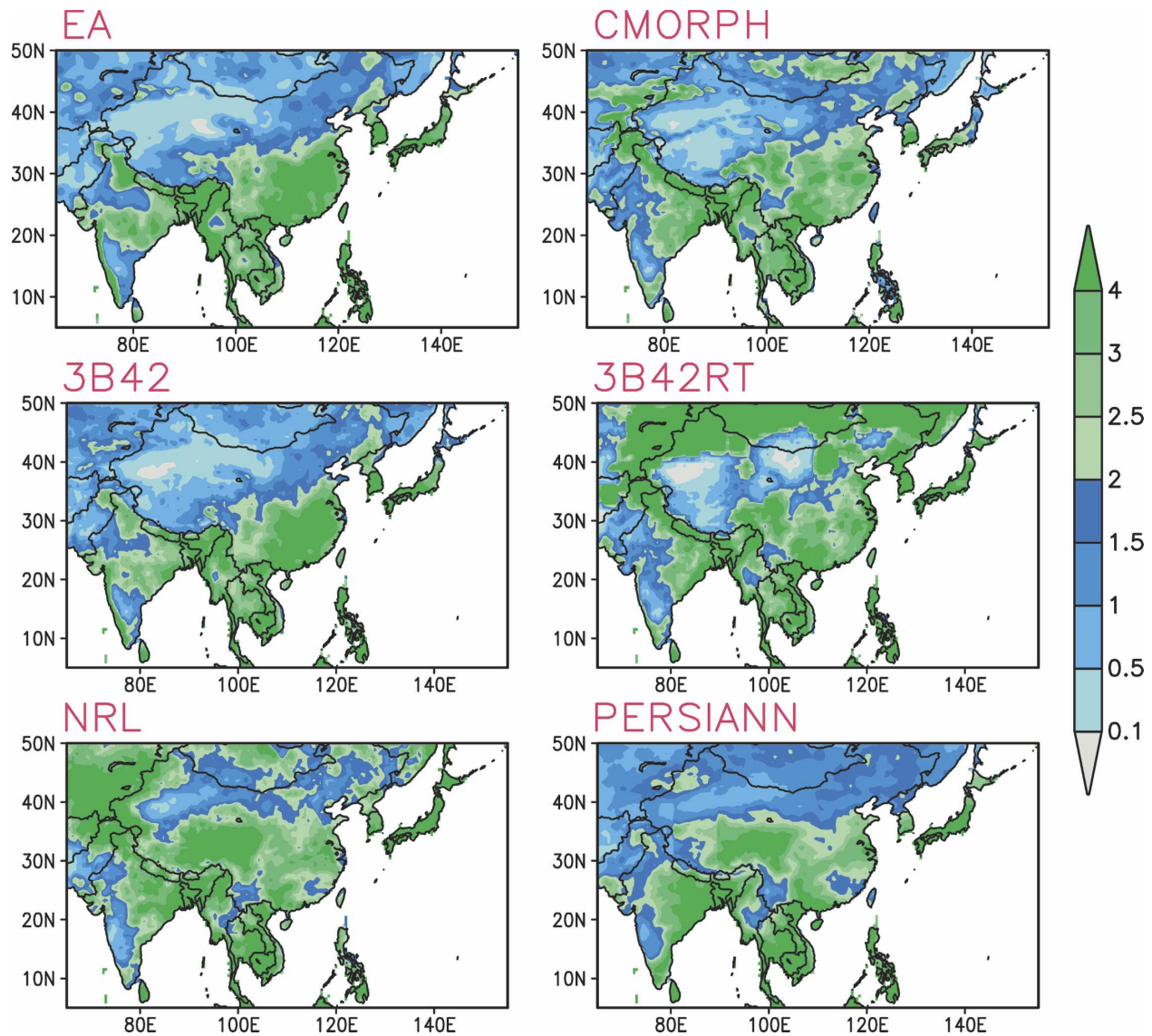


FIG. 10. Mean precipitation ( $\text{mm day}^{-1}$ ) for a 7-month period from January to July 2003, as obtained from the EA gauge-based analysis and satellite estimates of NOAA CPC CMORPH, NASA GSFC TRMM product 3B42, NRL precipitation product, and PERSIANN by the University of California, Irvin.

CMORPH technique, the surface snow/ice screening process is implemented using the daily snow/ice maps generated by the NOAA/National Environmental Satellite, Data, and Information Service (NESDIS). In the TRMM 3B42(RT), multichannel MW observations are employed to identify snow/ice contamination. No similar procedures are included in the NRL and PERSIANN techniques to be compared here. All these factors (differences in input datasets and quality control procedures) may influence the performance of the fine-resolution satellite precipitation estimates. Cautions therefore are needed in interpreting the examination results shown in the following discussions.

To examine the performance of the five products described above, daily precipitation estimates are calculated on a  $0.5^\circ$  latitude–longitude grid over the East Asia domain for a 7-month period from January to July 2003 for which the gauge analysis and all of the five satellite datasets are available. Comparisons are then conducted with our gauge-based analysis. Figure 10 shows the spatial distribution of the 7-month mean precipitation from the EA gauge analysis and the five satellite datasets. Heavy rainfall is observed over Japan, southern Korea, southeastern China, the Philippines, Southeast Asia, Western Ghats, and the southern slope of Himalaya, while only a very limited amount of pre-

precipitation is observed over the northern half of our target domain. All of the five satellite products captured the overall spatial structure of precipitation variations reasonably well. Among the four products based solely on satellite observations, CMORPH exhibits excellent skills in depicting the spatial patterns of precipitation, especially those associated with orographic effects (e.g., over northwestern China), but tends to underestimate the precipitation amount over eastern China and the Western Ghats. The NRL and PERSIANN generate a huge mass of precipitation over the Tibet Plateau that is not visible in the gauge-based analysis, while they miss the narrow band of rainfall along the Western Ghats caused by orographic forcing. Substantial overestimates of precipitation are observed with the TRMM 3B42RT over a northern portion of the data domain covering northwestern China, Mongolia, and northeastern China. A brief examination (not shown) revealed that the overestimation was caused by undesirable definition in the then-current version of the code for the estimation coefficients from IR data over cold surface when MW observations are unavailable. The problem was fixed in early March 2003 and the magnitude of precipitation estimates over the region in the later version of 3B42RT becomes reasonable compared to the gauge observations from March 2003. Adjusted against the GPCP monthly gauge data, the TRMM 3B42, meanwhile, presents the closest magnitude agreements with our EA gauge analysis over the entire domain.

Quantitative examinations are performed for the satellite products over China where our gauge analysis is derived from a dense station network. As shown in Fig. 11, skills are better over the eastern half of the country for all of the five satellite-based products in representing temporal variations of daily precipitation. Among the four satellite-only products, CMORPH stands out in capturing the temporal variations of precipitation. Serial correlation for CMORPH exceeds 0.6 over most of the region, while it is between 0.4 and 0.6 for TRMM 3B42RT, NRL, and PERSIANN. Adjustment against the GPCP gauge data yielded much higher correlation for the TRMM 3B42, an improvement achieved at least partially through reducing temporally and regionally dependent bias in the unadjusted satellite-only products.

Except for several small regions (e.g., over the northwestern corner of the country), correlation is generally low over western China for all of the satellite products, with close to zero correlation computed over the northern part of the Tibet Plateau and the Taklimakan Desert over western China. The low correlation spreads widely over western China regardless of the local gauge network density shown in Fig. 2, suggesting

that it is less attributable to the degraded gauge analysis over the region. Comparing with the mean precipitation distribution in Fig. 10, it seems that the satellite algorithms examined here tend to perform better over regions with wetter climate, while they demonstrate limited skills over arid and semiarid areas. Our findings here are in agreement with those of Ebert et al. (2007) and Turk et al. (2006) based on examinations over Australia and the United States.

The satellite precipitation products present better quantitative accuracy during warm seasons than during cold seasons (Fig. 12). Pattern correlation for CMORPH and TRMM 3B42 is  $\sim 0.75$  and  $\sim 0.50$ , during summer and winter, respectively. The CMORPH outperforms the other three satellite-only products (TRMM 3B42RT, NRL, and PERSIANN) consistently through most of the 7-month comparison period, while the gauge-adjusted TRMM 3B42 presents similar pattern correlation and a slightly smaller bias compared to the CMORPH. Degradation in pattern correlation observed for the NRL precipitation is largely caused by the poor sampling of IR data used to define the precipitation estimates. An inspection of the data files found that 3-hourly precipitation fields used to define the daily mean are available for only 68% of the time slots during the 7 months. In particular, for the period during June 2003, only two slots of 3-hourly precipitation estimates are available to define the daily values during that period in the NRL.

All of the five satellite products examined here reproduced the day-to-day variations of precipitation reasonably well. As shown in Fig. 13, the occurrences of the precipitation events associated with the Mei-Yu (Baiu) monsoon system over eastern China are very well captured by all of the five products. The magnitude of the peak precipitation, however, is not estimated very well, with the gauge-corrected TRMM 3B42 presenting the closest agreement with the gauge-based analysis.

Overall, among the four products based solely on satellite observations, CMORPH exhibits the highest skills in estimating spatial distribution and temporal variations of precipitation over China (Table 2). The comparison results presented in this study for East Asia are in qualitative agreements with those reported by Ebert et al. (2007) for the continental United States and Australia.

As described earlier in this section, part of the differences in the performance of the satellite products is attributable to the differing input satellite datasets, especially the microwave-based precipitation estimates, used by various authors. The NRL and the PERSIANN products examined in this paper are precipitation esti-

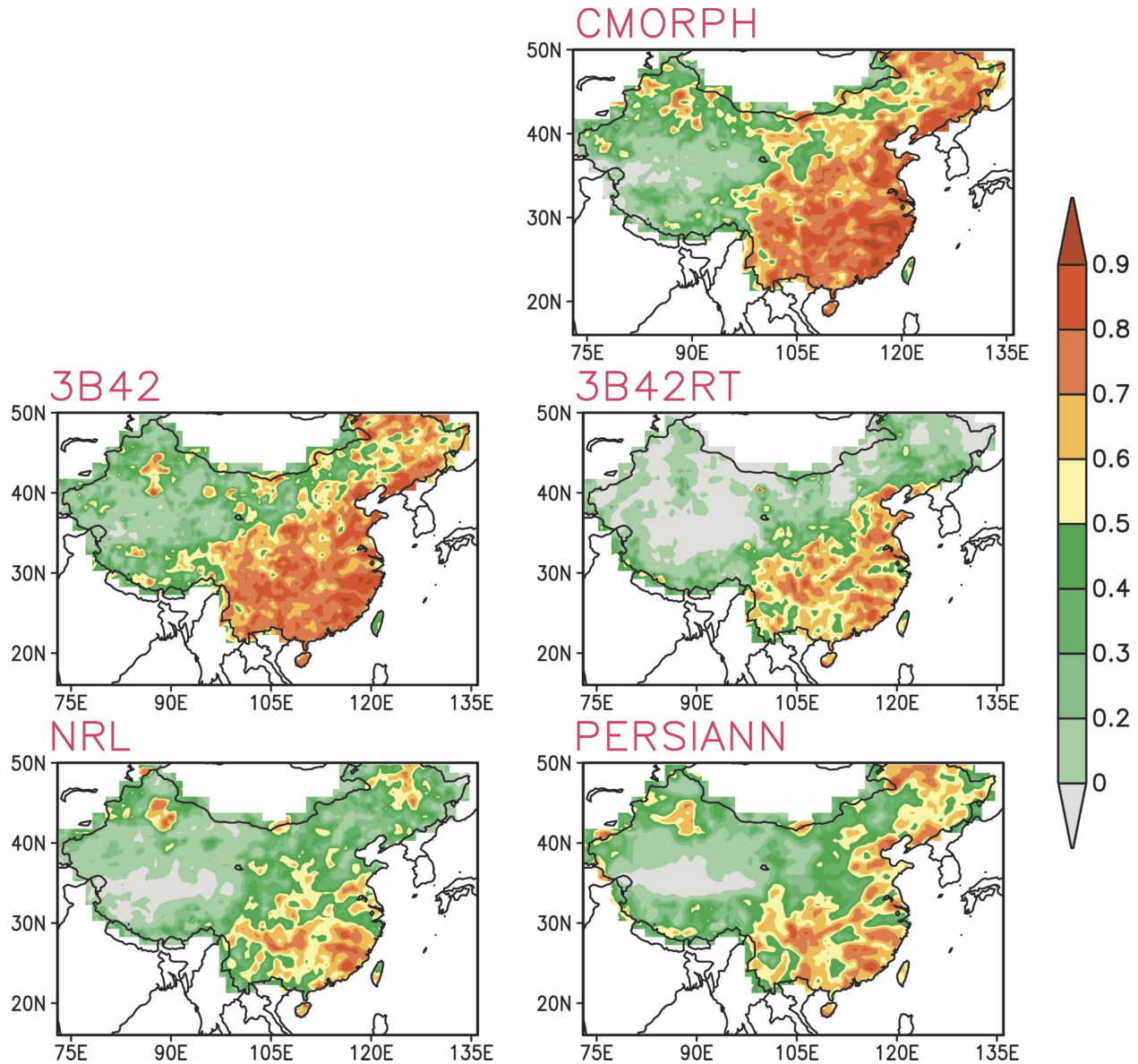


FIG. 11. Serial correlation between the East Asia gauge-based daily precipitation analysis and satellite estimates of CMORPH, TRMM 3B42, NRL, and PERSIANN at a 0.5° latitude-longitude grid box for a 7-month period from January to July of 2003.

mates derived from IR observations calibrated against MW observations from TMI, SSM/I, and AMSU (for NRL only). The TRMM 3B42RT is a merged analysis of the IR-based estimates with MW-based estimates derived from TMI and SSM/I. The CMORPH, meanwhile, takes information from TMI, SSM/I, as well as the AMSU.

Huge overestimates of precipitation observed with the NRL and the PERSIANN over the Tibet Plateau and northern China during winter and spring may be caused by contaminations of ground snow/ice in the MW-based estimates used to train the IR data. Daily

snow maps of NOAA/NESDIS, meanwhile, are used in the CMORPH to identify MW pixels atop a surface with snow cover (Joyce et al. 2004).

TRMM 3B42 is derived from an all-satellite product similar to 3B42RT, and the better comparison statistics for the 3B42 are attributable to both the bias correction procedure and the increased number of MW-based precipitation estimates included than those in the 3B42RT. The outstanding statistics for 3B42, however, suggest that adjusting the satellite estimates against gauge data improves both the magnitude and pattern agreements of the precipitation product. No such gauge-

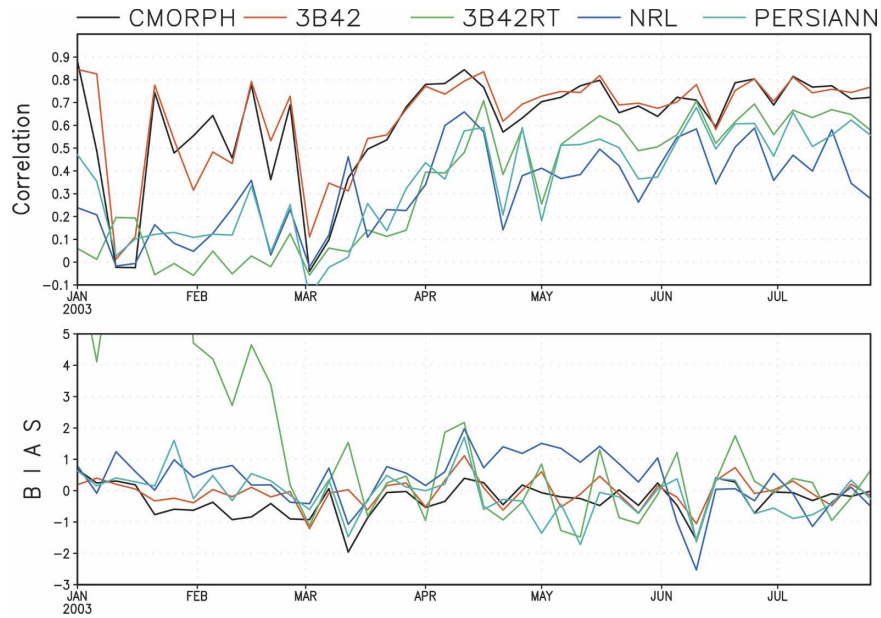


FIG. 12. Time series of pattern correlation between the East Asia gauge-based daily precipitation analysis and satellite estimates based on CMORPH (black), TRMM 3B42 (red), TRMM 3B42RT (green), NRL (blue), and PERSIANN (cyan). Pattern correlation is calculated for the domain of China. Only the data over a  $0.5^\circ$  latitude–longitude grid box where/when daily precipitation reports are available from one or more gauges and satellite estimates are generated from all four products.

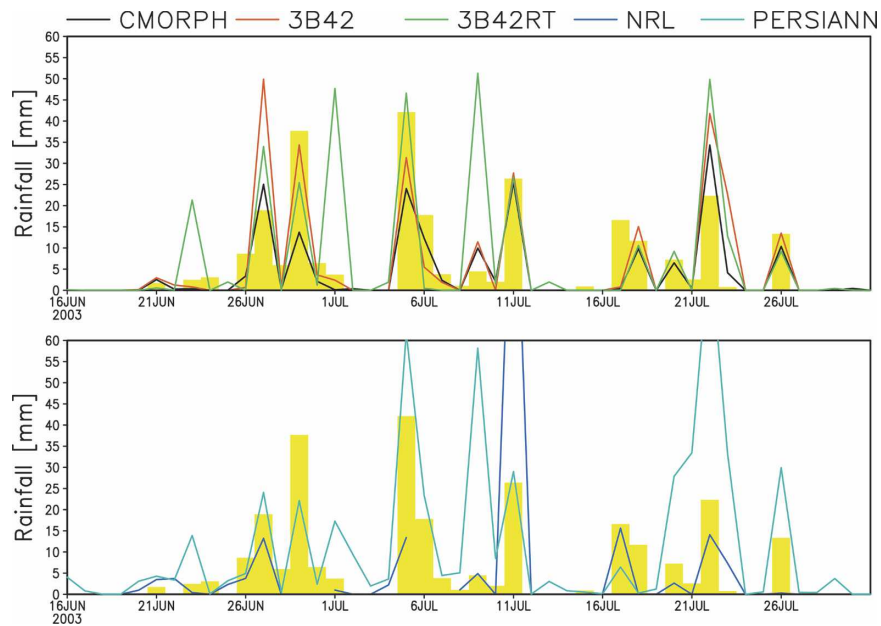


FIG. 13. Time series of daily precipitation for a period of 16 Jun to 31 Jul 2003 over a  $0.5^\circ$  latitude–longitude grid box centered at  $31.25^\circ\text{N}$ ,  $120.25^\circ\text{E}$  over eastern China for the gauge-based analysis (bar) and satellite estimates of (top) CMORPH (black), (top) TRMM 3B42 (red), (top) TRMM 3B42RT (green), (bottom) NRL (blue), and (bottom) PERSIANN (cyan).

TABLE 2. Results of comparison with fine-resolution satellite precipitation estimates over China for a 7-month period from January to July 2003. Comparisons are conducted over grid boxes with at least one gauge. Cold and warm seasons are from January to March and April to July 2003, respectively. Gauge-observed mean precipitation for the cold and warm seasons and the entire data period is 0.84, 3.61, and 2.52 mm day<sup>-1</sup>, respectively.

Satellite product	Cold season		Warm season		Entire period	
	Bias	Corr.	Bias	Corr.	Bias	Corr.
CMORPH	-0.38	0.504	-0.20	0.750	-0.27	0.745
3B42	-0.05	0.647	-0.07	0.758	-0.06	0.756
3B42RT	4.56	0.002	-0.07	0.585	1.75	0.312
NRL	0.39	0.153	0.31	0.445	0.34	0.438
PERSIANN	0.22	0.207	-0.37	0.557	-0.14	0.549

based adjustments are implemented with the NRL, the PERSIANN, and the CMORPH estimates examined in this study. Further improvements are expected with these techniques when similar adjustment procedures are included to remove the bias in the satellite estimates.

Techniques to generate blended products of fine-resolution precipitation estimates are relatively new and evolved rapidly in recent years. A series of improvements have been made to the products described in this section since the time period of 2003 for which our comparison is conducted. Starting from January 2004, the NRL adopted a new way to define the final precipitation fields as a weighted mean of the IR-based estimates as examined in this study and the MW-based estimates, which were only used for calibration of IR data in the old version (Turk and Miller 2005). In the new NRL algorithm, the weight for the MW estimates is set to unity, while that of the IR-based estimates is variable between 0 and 1 to reflect the regional and seasonal dependence of their performance. For the TRMM 3B42(RT), two major changes have been made at 2 March 2003 and 15 April 2004 to refine the IR calibration over cold land areas (Huffman et al. 2007). Details of changes in the techniques up to 2005 may be found in Turk and Bauer (2005) and Turk et al. (2006). Because of these changes, the comparison results presented in this section do not necessarily reflect the current state of the algorithms.

It is important to examine the evolution of the performance of these satellite precipitation products for regions where gauge data are available for such practices. Such efforts are being conducted by Ebert et al. (2007) on a real-time basis for the United States and Australia ([www.cpc.ncep.noaa.gov/products/janowiak/us\\_web.shtml](http://www.cpc.ncep.noaa.gov/products/janowiak/us_web.shtml)) and by C. Kidd for western Europe ([kermit.bham.ac.uk/~ipwgeu](http://kermit.bham.ac.uk/~ipwgeu)). In addition, a new project, Program to Evaluate High Resolution Precipitation

Products (PEHRPP), has been initiated recently as part of the International Precipitation Working Group (IPWG) activities to provide a platform for comprehensive evaluations of the satellite products (<http://www.isac.cnr.it/~ipwg/IPWG.html>). For the East Asia region, we will continue our examinations for recent years when station data are available and the gauge-based analysis is updated.

## 5. Summary

An analysis of daily precipitation has been constructed on a 0.5° latitude–longitude grid over East Asia (5°–60°N, 65°–155°E) for a 26-yr period from 1978 to 2003 by interpolating station observations at over 2200 gauges collected from several individual sources. First, daily climatology is defined for each station as the summation of the first six harmonics for the 365-calendar day time series of the mean daily values averaged over a 20-yr period from 1978 to 1997. Analyzed fields of daily precipitation climatology are then created by interpolating the truncated station climatology through the algorithm of Shepard (1968). To account for the orographic effects, these fields are then adjusted by the PRISM monthly precipitation climatology of Daly et al. (1994) and Daly et al. (2002) so that the monthly accumulation of the daily climatology meets that of the PRISM, while temporal variation patterns in the original daily climatology time series are retained. Analyzed fields of ratio of daily precipitation to daily climatology are created by interpolating the corresponding station values through the optimal interpolation (OI) technique of Gandin (1965). Analyses of total daily precipitation are finally calculated by multiplying the daily climatology with the daily ratio.

Cross-validation tests are conducted to examine the quantitative accuracy of the new daily analyses. The results showed that the correlation between the analyses and the withdrawn gauge data is ~0.6 and the bias is almost zero. Performance of the gauge-based analyses improves as the gauge network density, with correlation reaching above 0.8 over the Yellow River basin where a very dense gauge network is available. Derived from observations over many more gauges and using an improved algorithm with orographic consideration, our new analysis presents precipitation variations with finer spatial structures compared to existing gauge-based datasets. Magnitude of precipitation in our EA analysis is generally slightly larger than that in other published products.

Our new EA analysis is applied to verify satellite-estimated daily precipitation fields over China for a 7-month period from January to July 2003. Overall, all

satellite products examined here present reasonable skill in representing the spatial distributions and temporal variations of precipitation over China. All the satellite products exhibit better performance in depicting precipitation for regions and seasons of wet climate. Only limited skills are achieved by the satellite algorithms in estimating precipitation over arid and semi-arid regions over central Asia.

The work reported here is an integral part of our long-term effort to construct fine-resolution precipitation analyses over East Asia. Further improvements of the gauge-based analysis are underway to include gauge observations from more stations, to refine the orographic effect correction procedures for areas without PRISM, and to add in bias correction for the wind effects through employment of published correction coefficients (e.g., Legates and Willmott 1990; Ye et al. 2004). Our emphasis here is to improve the quantitative accuracy of our gauge-based analysis over South and Southeast Asia where heavy precipitation with significant orographic enhancements is observed by a less desirable gauge network of GTS in the current version of our EA gauge analysis. The gauge-based daily precipitation dataset described in this paper is available to all interested scientists. We welcome collaborations in improving this analysis by refining the algorithm and including more gauge data.

*Acknowledgments.* The authors thank Dr. X. Ma who collected and kindly provided the hydrological station precipitation data used in this study. The daily precipitation data over ~700 Chinese stations are collected and quality controlled by the Chinese Meteorological Administration (CMA). The PRISM monthly precipitation climatology over China and Mongolia is provided by Dr. C. Daly of Oregon State University. Comments and suggestions by J. E. Janowiak, Y. Fan, G. Huffman, P. A. Arkin, J. Turk, B. Ebert, D. Bolvin, and the anonymous reviewers greatly improved our original manuscript. This project is part of a joint effort among the NOAA Climate Prediction Center (CPC), the Research Institute for Humanity and Nature (RIHN) of Japan, and the Institute for Geographical Sciences and Natural Resources Research (IGSNRR) of the Chinese Academy of Science. The research work of RIHN is partly supported by the Global Environmental Research Fund (Fs-051 and B-062) by the Ministry of the Environment of Japan.

#### REFERENCES

- Adam, J. C., and D. P. Lettenmaier, 2003: Adjustment of global gridded precipitation for systematic bias. *J. Geophys. Res.*, **108**, 4257, doi:10.1029/2002JD002499.
- , E. A. Clark, D. P. Lettenmaier, and E. F. Wood, 2006: Correction of global precipitation products for orographic effects. *J. Climate*, **19**, 15–38.
- Adler, R. F., C. Kidd, G. Petty, M. Morrissey, and H. M. Goodman, 2001: Intercomparison of global precipitation products: The third Precipitation Intercomparison Project (PIP-3). *Bull. Amer. Meteor. Soc.*, **82**, 1377–1396.
- , and Coauthors, 2003: The Version 2 Global Precipitation Climatology Project (GPCP) monthly precipitation analysis (1979–present). *J. Hydrometeorol.*, **4**, 1147–1167.
- Arkin, P. A., and B. N. Meisner, 1987: The relationship between large-scale convective rainfall and cold cloud cover over the western hemisphere during 1982–1984. *Mon. Wea. Rev.*, **115**, 51–74.
- Bradley, R. S., H. F. Diaz, J. K. Eischeid, P. D. Jones, P. M. Kelly, and C. M. Goodess, 1987: Precipitation fluctuations over Northern Hemisphere land areas since the mid-19th century. *Science*, **237**, 171–175.
- Bussières, N., and W. Hogg, 1989: The objective analysis of daily rainfall by distance weighting schemes on a mesoscale grid. *Atmos.–Ocean*, **27**, 521–541.
- Chen, M., P. Xie, J. E. Janowiak, and P. A. Arkin, 2002: Global land precipitation: A 50-year monthly analysis based on gauge observations. *J. Hydrometeorol.*, **3**, 249–266.
- , —, —, and —, 2004: Orographic enhancements in precipitation: An intercomparison of two gauge-based precipitation climatologies. Preprints, *18th Conf. on Hydrology*, Seattle, WA, Amer. Meteor. Soc., CD-ROM, 5.1.
- Creutin, J. D., and C. Obled, 1982: Objective analysis and mapping techniques for rainfall fields: An objective comparison. *Water Resour. Res.*, **18**, 413–431.
- Dai, A., and T. M. L. Wigley, 2000: Global patterns of ENSO-induced precipitation. *Geophys. Res. Lett.*, **27**, 1283–1286.
- , I. Y. Fung, and A. D. del Genio, 1997: Surface observed global land precipitation variations during 1900–88. *J. Climate*, **10**, 2943–2962.
- Daly, C., R. P. Neilson, and D. L. Phillips, 1994: A statistical-topographic model for mapping climatological precipitation over mountainous terrain. *J. Appl. Meteor.*, **33**, 140–158.
- , W. P. Gibson, G. H. Taylor, G. L. Johnson, and P. Pasteris, 2002: A knowledge-based approach to the statistical mapping of climate. *Climate Res.*, **22**, 99–113.
- Ebert, E. E., and M. J. Manton, 1998: Performance of satellite rainfall estimation algorithms during TOGA COARE. *J. Atmos. Sci.*, **55**, 1537–1557.
- , J. E. Janowiak, and C. Kidd, 2007: Comparison of near-real-time precipitation estimates from satellite observations and numerical models. *Bull. Amer. Meteor. Soc.*, **88**, 47–64.
- Eischeid, J. K., H. F. Diaz, R. S. Bradley, and P. D. Jones, 1991: A comprehensive precipitation dataset for global land areas. U.S. Department of Energy Tech. Rep. DOE/ER-6901T-H1, 81 pp. [Available from National Technical Information Services, U.S. Department of Commerce, Springfield, VA 22161.]
- Fekete, B. M., C. J. Vorosmarty, J. O. Roads, and C. J. Willmott, 2004: Uncertainties in precipitation and their impacts on runoff estimates. *J. Climate*, **17**, 294–304.
- Ferraro, R. R., 1997: Special sensor microwave imager derived global rainfall estimates for climatological applications. *J. Geophys. Res.*, **102**, 16 715–16 735.
- Frei, C., and C. Schär, 1998: A precipitation climatology of the Alps from high-resolution rain-gauge observations. *Int. J. Climatol.*, **18**, 873–900.

- Gandin, L. S., 1965: *Objective Analysis of Meteorological Fields*. Israel Program for Scientific Translations, 242 pp.
- Gleason, B. E., 2002: The Global Daily Climatology Network (GDCN), version 1.0. NOAA/NCDC data documentation for data set 9101. [Available online at <http://www.ncdc.noaa.gov/oa/climate/research/gdcn/gdcn.html>.]
- Higgins, R. W., W. Shi, E. Yarosh, and R. Joyce, 2000: Improved United States precipitation quality control system and analysis. *NCEP/Climate Prediction Center Atlas*, No. 7, National Oceanic and Atmospheric Administration, National Weather Service. [Available online at [http://www.cpc.ncep.noaa.gov/research\\_papers/ncep\\_cpc\\_atlas/7/index.html](http://www.cpc.ncep.noaa.gov/research_papers/ncep_cpc_atlas/7/index.html).]
- Hsu, K.-L., X. Gao, S. Sorooshian, and V. Gupta, 1997: Precipitation estimation from remotely sensed information using artificial neural networks. *J. Appl. Meteor.*, **36**, 1176–1190.
- Huffman, G. J., and Coauthors, 1997: The Global Precipitation Climatology Project (GPCP) combined precipitation dataset. *Bull. Amer. Meteor. Soc.*, **78**, 5–20.
- , R. F. Adler, M. M. Morrissey, D. T. Bolvin, S. Curtis, R. Joyce, B. McGavock, and J. Susskind, 2001: Global precipitation at one-degree daily resolution from multisatellite observations. *J. Hydrometeorol.*, **2**, 36–50.
- , —, E. F. Stocker, D. T. Bolvin, and E. J. Nelkin, 2004: Analysis of TRMM 3-hourly multi-satellite precipitation estimates computed in both real and post-real time. Preprints, *12th Conf. on Satellite Meteorology and Oceanography*, Long Beach, CA, Amer. Meteor. Soc., CD-ROM, P4.11.
- , —, D. T. Bolvin, G. Gu, E. J. Nelkin, K. P. Bowman, E. F. Stocker, and D. B. Wolff, 2007: The TRMM Multisatellite Precipitation Analysis (TMPA): Quasi-global, multiyear, combined-sensor precipitation estimates at fine scales. *J. Hydrometeorol.*, **8**, 38–55.
- Hulme, M., 1991: An intercomparison of model and observed global precipitation climatologies. *Geophys. Res. Lett.*, **18**, 1715–1718.
- , and M. G. New, 1997: Dependence of large-scale precipitation climatologies on temporal and spatial sampling. *J. Climate*, **10**, 1099–1113.
- Janowiak, J. E., and P. Xie, 1999: CAMS–OPI: A global satellite–rain gauge merged product for real-time precipitation monitoring applications. *J. Climate*, **12**, 3335–3342.
- , and —, 2003: A global-scale examination of monsoon-related precipitation. *J. Climate*, **16**, 4121–4133.
- , A. Gruber, C. R. Kondragunta, R. E. Livezey, and G. J. Huffman, 1998: A comparison of the NCEP–NCAR reanalysis precipitation and the GPCP rain gauge–satellite combined dataset with observational error considerations. *J. Climate*, **11**, 2960–2979.
- Joyce, R. J., J. E. Janowiak, P. A. Arkin, and P. Xie, 2004: CMORPH: A method that produces global precipitation estimates from passive microwave and infrared data at high spatial and temporal resolution. *J. Hydrometeorol.*, **5**, 487–503.
- Kummerow, C., and Coauthors, 2000: The status of the Tropical Rainfall Measuring Mission (TRMM) after two years in orbit. *J. Appl. Meteor.*, **39**, 1965–1982.
- Lau, K.-M., and H. T. Wu, 2001: Principal modes of rainfall–SST variability of the Asian summer monsoon: A reassessment of the monsoon–ENSO relationship. *J. Climate*, **14**, 2880–2895.
- Legates, D. R., and C. J. Willmott, 1990: Mean seasonal and spatial variability in gauge-corrected, global precipitation. *Int. J. Climatol.*, **10**, 111–127.
- Liu, C., and H. Zheng, 2004: Changes in components of the hydrological cycle in the Yellow River basin during the second half of the 20th century. *Hydrol. Process.*, **18**, 2337–2345.
- Ma, X., and Y. Fukushima, 2002: Numerical model of river flow formation from small to large scale river basins. *Mathematical Models of Watershed Hydrology*, V. P. Singh and D. K. Frevert, Eds., Water Resources Publications, 433–470.
- McCollum, J., W. F. Krajewski, R. R. Ferraro, and M. B. Ba, 2002: Evaluation of biases of satellite rainfall estimation algorithms over the continental United States. *J. Appl. Meteor.*, **41**, 1065–1080.
- Morrissey, M. L., M. A. Shafer, S. E. Postawko, and B. Gibson, 1995a: The Pacific rain gauge rainfall database. *Water Resour. Res.*, **31**, 2111–2113.
- , J. A. Maliekal, J. S. Greene, and J. Wang, 1995b: The uncertainty of simple averages using rain gauge networks. *Water Resour. Res.*, **31**, 2011–2017.
- New, M., M. Hulme, and P. Jones, 1999: Representing twentieth-century space–time climate variability. Part I: Development of a 1961–90 mean monthly terrestrial climatology. *J. Climate*, **12**, 829–856.
- , —, and —, 2000: Representing twentieth-century space–time climate variability. Part II: Development of 1901–96 monthly grids of terrestrial surface climate. *J. Climate*, **13**, 2217–2238.
- Nijssen, B., G. M. O’Donnell, and D. P. Lettenmaier, 2001: Predicting the discharge of global rivers. *J. Climate*, **14**, 3307–3323.
- Roads, J. O., S. C. Chen, and F. Fujioka, 2001: ECPC’s weekly to seasonal global forecasts. *Bull. Amer. Meteor. Soc.*, **82**, 639–658.
- Ropelewski, C. F., J. E. Janowiak, and M. S. Halpert, 1985: The analysis and display of real-time surface climate data. *Mon. Wea. Rev.*, **113**, 1101–1106.
- Rubel, F., and M. Hantel, 2001: BALTEX 1/6-degree daily precipitation climatology 1996–1998. *Meteor. Atmos. Phys.*, **77**, 155–166.
- Rudolf, B., 1993: Management and analysis of precipitation data on a routine basis. *Proc. Int. Symp. on Precipitation and Evaporation*. Bratislava, Slovakia, WMO, 69–76.
- Schaake, J., A. Henkel, and S. Cong, 2004: Application of PRISM climatologies for hydrologic modeling and forecasting in the western U.S. Preprints, *18th Conf. on Hydrology*, Seattle, WA, Amer. Meteor. Soc., CD-ROM, 5.3.
- Schneider, U., 1993: The GPCC quality-control system for gauge-measured precipitation data. *Proc. Analysis Methods for Precipitation on a Global Scale: Report of a GEWEX Workshop*, WCRP-81, WMO/TD-588, Koblenz, Germany, GPCC, A5–A9.
- Sevruk, B., 1982: Methods of correction for systematic error in point precipitation measurement for operational use. *Operational Hydrology Rep.* 21, WMO Rep. 589, 91 pp.
- Shepard, D., 1968: A two dimensional interpolation function for irregularly spaced data. *Proc. 23d National Conf. of the Association for Computing Machinery*, Princeton, NJ, ACM, 517–524.
- Shi, W., R. W. Higgins, E. Yarosh, and V. E. Kousky, 2001: The annual cycle and variability of precipitation in Brazil. *NCEP/Climate Prediction Center Atlas*, No. 9, National Oceanic and Atmospheric Administration, National Weather Service. [Available online at [http://www.cpc.ncep.noaa.gov/research\\_papers/ncep\\_cpc\\_atlas/9/index.html](http://www.cpc.ncep.noaa.gov/research_papers/ncep_cpc_atlas/9/index.html).]
- Sorooshian, S., K.-L. Hsu, X. Gao, H. V. Gupta, B. Imam, and D. Braithwaite, 2000: Evaluation of PERSIANN system satel-

- lite-based estimates of tropical rainfall. *Bull. Amer. Meteor. Soc.*, **81**, 2035–2046.
- Spencer, R. W., 1993: Global oceanic precipitation from MSU during 1979–91 and comparisons to other climatologies. *J. Climate*, **6**, 1301–1326.
- Su, F. G., J. C. Adam, L. C. Bowling, and D. P. Lettenmaier, 2005: Streamflow simulation of the terrestrial Arctic domain. *J. Geophys. Res.*, **110**, D08112, doi:10.1029/10.1029/2004JD005518.
- Susskind, J., P. Piraino, L. Rokkle, and A. Mehta, 1997: Characteristics of the TOVS Pathfinder Path A dataset. *Bull. Amer. Meteor. Soc.*, **78**, 1449–1472.
- Trenberth, K. E., and J. M. Caron, 2000: The Southern Oscillation revisited: Sea level pressures, surface temperatures, and precipitation. *J. Climate*, **13**, 4358–4365.
- Turk, F. J., and P. Bauer, Eds., 2005: Second International Precipitation Working Group Workshop. EUMETSAT Publication EUM P.44, 355 pp. [Available from EUMETSAT, Am Kavalleriesand 31, D-64295 Darmstadt, Germany.]
- , and S. D. Miller, 2005: Toward improved characterization of remotely sensed precipitation regimes with MODIS/AMSR-E blended data technique. *IEEE Trans. Geosci. Remote Sens.*, **43**, 1059–1069.
- , E. E. Ebert, B.-J. Sohn, H.-J. Oh, V. Levizzani, E. A. Smith, and R. Ferraro, 2004: Validation of an operational global precipitation analysis at short time scales. Preprints, *12th Conf. on Satellite Meteorology and Oceanography*, Long Beach, CA, Amer. Meteor. Soc., CD-ROM, J1.2.
- , P. Bauer, E. Ebert, and P. A. Arkin, 2006: Satellite-derived precipitation verification activities within the International Precipitation Working Group (IPWG). *14th Conf. on Satellite Meteorology and Oceanography*, Atlanta, GA, Amer. Meteor. Soc., CD-ROM, P2.15.
- Vose, R. S., R. L. Schmoyer, P. M. Steurer, T. C. Peterson, R. Heim, T. R. Karl, and J. K. Eischeid, 1992: The Global Historical Climatology Network: Long-term monthly temperature, precipitation, sea-level pressure, and station pressure data. Tech. Rep. ORNL/CDIAC-53, Oak Ridge National Laboratory/Carbon Dioxide Information Analysis Center, Oak Ridge, TN, 26 pp.
- Weymouth, G., G. A. Mills, D. Jones, E. E. Ebert, and M. J. Manton, 1999: A continental-scale daily rainfall analysis system. *Aust. Meteor. Mag.*, **48**, 169–179.
- Wilheit, T. J., A. T. C. Chang, and L. S. Chiu, 1991: Retrieval of monthly rainfall indices from microwave radiometric measurements using probability distribution functions. *J. Atmos. Oceanic Technol.*, **8**, 118–136.
- Willmott, C. J., and K. Matsuura, 1995: Smart interpolation of annually averaged air temperature in the United States. *J. Appl. Meteor.*, **34**, 2577–2586.
- , S. M. Robeson, and M. J. Janis, 1996: Comparison of approaches for estimating time-averaged precipitation using data from the USA. *Int. J. Climatol.*, **16**, 1103–1115.
- Xie, P., and P. A. Arkin, 1997: Global precipitation: A 17-year monthly analysis based on gauge observations, satellite estimates, and numerical model outputs. *Bull. Amer. Meteor. Soc.*, **78**, 2539–2558.
- , and —, 1998: Global monthly precipitation estimates from satellite-observed outgoing longwave radiation. *J. Climate*, **11**, 137–164.
- , B. Rudolf, U. Schneider, and P. A. Arkin, 1996: Gauge-based monthly analysis of global land precipitation from 1971 to 1994. *J. Geophys. Res.*, **101** (D14), 19 023–19 034.
- , J. E. Janowiak, P. A. Arkin, R. Adler, A. Gruber, R. Ferraro, G. J. Huffman, and S. Curtis, 2003: GPCP pentad precipitation analyses: An experimental dataset based on gauge observations and satellite estimates. *J. Climate*, **16**, 2197–2214.
- Xue, Y., and Coauthors, 2005: Multiscale variability of the river runoff system in China and its long-term link to precipitation and sea surface temperature. *J. Hydrometeorol.*, **6**, 550–570.
- Yatagai, A., P. Xie, and A. Kitoh, 2005: Utilization of a new gauge-based daily precipitation dataset over monsoon Asia for validation of the daily precipitation climatology simulated by the MRI/JMA 20-km-mesh AGCM. *Sci. Online Lett. Atmos.*, **1**, 193–196.
- Ye, B., D. Yang, Y. Ding, and T. Han, 2004: A bias-corrected precipitation climatology for China. *J. Hydrometeorol.*, **5**, 1147–1160.